

The TAOS Project Stellar Variability I. Detection of Low-Amplitude δ Scuti Stars

D.-W. Kim^{1,2,3}, P. Protopapas^{1,2}, C. Alcock¹, Y.-I. Byun³, J. Kyeong⁴, B.-C. Lee⁴, N. J. Wright¹, T. Axelrod⁵, F. B. Bianco^{1,6}, W.-P. Chen⁷, N. K. Coehlo⁸, K. H. Cook⁹, R. Dave², S.-K. King¹⁰, T. Lee¹⁰, M. J. Lehner^{10,6,1}, H.-C. Lin⁷, S. L. Marshall^{9,11}, R. Porrata¹², J. A. Rice⁸, M. E. Schwamb¹³, J.-H. Wang^{7,10}, S.-Y. Wang¹⁰, C.-Y. Wen¹⁰ and Z.-W. Zhang^{7,10}

ABSTRACT

We analyzed data accumulated during 2005 and 2006 by the Taiwan-American Occultation Survey (TAOS) in order to detect short-period variable stars (periods of $\lesssim 1$ hour) such as δ Scuti. TAOS is designed for the detection of stellar occultation by small-size Kuiper Belt Objects (KBOs) and is operating four 50cm telescopes at an effective cadence of 5Hz. The four telescopes simultaneously monitor the same patch of the sky in order to reduce false positives. To detect short-period variables, we used the Fast Fourier Transform algorithm (FFT) inasmuch as the data points in TAOS light-curves are evenly spaced. Using FFT, we found 41 short-period variables with amplitudes smaller than a few hundredths of a magnitude and periods of about an hour, which suggest that they are low-amplitude δ Scuti stars (LADS). The light-curves of TAOS δ Scuti stars are accessible online at the Time Series Center website (<http://timemachine.iic.harvard.edu>).

Subject headings: (stars: variables:) δ Sct; surveys; methods : data analysis

1. INTRODUCTION

δ Scuti stars (hereinafter, δ Sct stars) are pulsating variables inside the classical instability strip and on or close to the main-sequence. They are typically placed at

the lower on the instability strip than RR Lyrae stars or Cepheids and thus they are fainter than RR Lyrae stars or Cepheids. Their spectral types are between A and late F. Their periods are between ~ 0.02 days and ~ 0.25 days, which is relatively shorter than other types of variables (e.g. γ Dor; Henry et al. (2001)). Based on these characteristics, δ Sct stars can be separated from other types of variable stars such as RR Lyrae, β Cepheid, γ Dor etc (Breger 2000a).

The majority of the δ Sct stars are low-amplitude δ Sct stars (LADS) with amplitudes from a milli-magnitude to a few tens of milli-magnitude. LADS are mainly non-radial p-mode pulsators (Breger 2000a). Another subgroup of δ Sct stars is the high-amplitude δ Sct stars (HADS), whose amplitudes are bigger than ~ 0.3 magnitude. HADS are radial pulsators (Breger 2000a; Rodríguez et al. 1996). In addition to LADS and HADS, there is another interesting type pulsation star called SX Phe variable stars, which exhibit a type of pulsation similar to the δ Sct stars. They are relatively old and evolved Population II stars, whereas most of the δ Sct stars are Population I stars. Stellar evolutionary theory is not yet successful at explaining these SX Phe variable stars (Rodríguez & López-González 2000). Most of the SX Phe show similar properties with HADS such as high amplitude and short period. More detailed review of δ Sct stars is presented in Breger (2000a) (Breger 2000a) and references therein.

¹Harvard Smithsonian Center for Astrophysics, Cambridge, MA 02138

²Initiative in Innovative Computing, School of Engineering and Applied Sciences, Harvard, Cambridge, MA 02138

³Department of Astronomy, Yonsei University, Seoul, South Korea 120-749

⁴Korea Astronomy & Space Science Institute, Daejeon 305-348, Korea

⁵Steward Observatory, 933 North Cherry Avenue, Room N204 Tucson AZ 85721

⁶Department of Physics and Astronomy, University of Pennsylvania, 209 South 33rd Street, Philadelphia, PA 19104

⁷Institute of Astronomy, National Central University, No. 300, Jhongda Rd, Jhongli City, Taoyuan County 320, Taiwan

⁸Department of Statistics, University of California Berkeley, 367 Evans Hall, Berkeley, CA 94720

⁹Institute for Geophysics and Planetary Physics, Lawrence Livermore National Laboratory, Livermore, CA 94550

¹⁰Institute of Astronomy and Astrophysics, Academia Sinica, P.O. Box 23-141, Taipei 106, Taiwan

¹¹Kavli Institute for Particle Astrophysics and Cosmology, 2575 Sand Hill Road, MS 29, Menlo Park, CA 94025

¹²Department of Astronomy, University of California Berkeley, 601 Campbell Hall, Berkeley CA 94720

¹³Division of Geological and Planetary Sciences, California Institute of Technology, 1201 E. California Blvd., Pasadena, CA 91125

Because of their great number of radial and non-radial modes, it is known that δ Sct stars are suitable for asteroseismology research, which enables study of stellar interior structures (Brown & Gilliland 1994). For a better understanding of pulsating δ Sct stars and thus stellar structure, several authors studied δ Sct stars and detected their multiple frequencies of pulsation using either ground-based observations or space-based observations (Breger et al. 2002; Ripepi et al. 2003; Breger et al. 2005; Buzasi et al. 2005; Bruntt et al. 2007; Pribulla et al. 2008). Due to the better photometric precision, space-based observations data show better results on the analysis of multiple frequencies than ground-based observation data (Bruntt et al. 2007; Pribulla et al. 2008). However, some authors have pointed out that ground-based observations using multiple-site telescopes are still valuable because, with a baseline longer than space-based observations, they are useful for detecting long-period pulsation (for more details, see Breger et al. 2005; Bruntt et al. 2007 and references therein). Moreover, by parameterizing the amplitude ratio and the phase differences in different filters (e.g. *ubvy*), it is possible to derive the spherical harmonic degree, l (Garrido et al. 1990; Balona & Evers 1999; Moya et al. 2004), which is an important parameter for the asteroseismology studies. Therefore ground-based telescopes that are more feasible for multiple-site and multiple-filter observations (e.g. Delta Scuti Network, Zima et al. 2002) are nonetheless useful for the identification of pulsation modes and thus for the study of interior structures.

Another interesting feature of δ Sct stars is that some of them show period and amplitude variations (Breger & Pamyatnykh 1998; Breger 2000b; Arentoft et al. 2001). The period variation ($1/P$) dP/dt , based on observations, is about 10^{-7} per year for both period increases and decreases with equal distribution. On the other hand, theoretical models give ten times smaller period variation than observed; they also predict that period increases should be dominant over period decreases (Breger & Pamyatnykh 1998). Amplitude variations and time scales of the variations are different from star to star, ranging from a few milli-magnitudes to several tens of milli-magnitudes and from a few tens of days to a few hundreds of days (Arentoft et al. 2001). These period and amplitude variations are thought to be caused not by evolutionary effects but by some other mechanism (e.g. light-time effect because of the orbital motion in binaries or nonlinear mode interactions). However, the true origin of the variations is still unknown. For more details, see Breger & Pamyatnykh (1998) and references therein.

McNamara et al. (2007) investigated HADS in the Large Magellanic Cloud (LMC) and their period-luminosity (P-L) relation to test if they can be used as the standard distance candles. They found that the distance modulus for LMC derived using δ Sct stars is consistent with the distance moduli for LMC derived using RR Lyrae and

Cepheids, which implies the P-L relation of δ Sct stars can help to determine distances of *long-distance* objects such as objects in the LMC.

In this paper, we present the detection of 41 δ Sct candidate stars from the Taiwan-American Occultation Survey (TAOS) data accumulated during 2005 and 2006 observation (hereinafter, TAOS δ Sct stars). Among the 41 detections, there is one previously known ‘suspected variable’ star, NSV 3816, from the Suspected Variable stars and Supplement (Samus et al. 2009) (no period or type is provided in that catalog). The rest of the 40 TAOS δ Sct stars are newly detected by this study. Only 14 of the detected TAOS δ Sct stars have spectral types. Twelve of those have spectral types from A to F, which are typical for δ Sct stars. The remaining two have B8 and G5 spectral types, which are peculiar spectral types. Using spectroscopic instruments -BOES (Kim et al. 2007) and FAST (Fabricant et al. 1998)-, we obtained spectra for those two stars. As a result we found that the B8 star is an A5 star and the G5 star is an F0 star. Even though the rest of the detected stars do not have spectral type information, their low amplitudes, short periods and morphologies of light-curves strongly suggest that they are LADS.

In Section 2, we present a TAOS overview, data reduction processes and the detection algorithm we used to detect δ Sct stars in TAOS 2-year data. We provide a list of the detected TAOS δ Sct stars and their physical parameters (e.g. magnitude, period, amplitude, spectral type, etc) in Section 3. In Section 4, we present summaries.

2. TAOS δ Sct Stars

2.1. TAOS overview

TAOS aims to detect stellar occultations caused by small-sized Kuiper Belt Objects (KBOs) at a distance of Neptune’s orbit or beyond (Alcock et al. 2003; Chen et al. 2007; Lehner et al. 2009). Because of the short duration (< 1 sec) and the rareness of occultation events, TAOS monitors several hundreds of stars in a wide field of view (3 deg^2) with a high sampling rate. To reduce false positives, TAOS uses four 50 cm telescopes which simultaneously monitor the same patch of the sky. Due to the high sampling rate, TAOS data is also useful for detecting short-period variable stars such as δ Sct stars. Moreover, TAOS telescopes keep monitoring the same field up to 1.5 hours and can thus obtain full-phase light-curves of variable stars whose periods are shorter than 1.5 hours.

To detect such short-period variable stars, we analyzed TAOS data accumulated during 2005 and 2006. The dataset consists of 117 TAOS observation fields, which cover 351 deg^2 of the sky. It consists of ~ 200 runs, where

a run is a set of multiple (two or three¹) telescope observations for a given field and a given date. Note that the TAOS telescopes occasionally visit the same observation field multiple times according to the telescopes' observation schedules, which enables detecting the same variable stars multiple times. In such case, we are able to derive multiple frequencies of the stars as explained in Section 3.1.

2.2. Data Reduction

To detect periodic signals, we analyzed the light-curves generated by the TAOS photometry pipeline (Zhang et al. 2009). The pipeline was developed by the collaboration to extract light-curves of each star from *zipper images*. The *zipper images* are generated by the unique telescope operation mode called *zipper mode* which was developed in order to achieve high-speed photometry (Lehner et al. 2009).

After obtaining the light-curves using the TAOS photometry pipeline, we applied further cuts to the light-curves. Some of the individual measurements are flagged as invalid. This happens when the star moves out of the field of view because of temporary telescope vibrations or tracking error, thus yielding no photometrical measurements. We therefore applied a B-spline (de Boor 1978) and replaced the flagged measurements with values interpolated from the spline fit. After the interpolation process, in order to increase the signal-to-noise ratio (SNR), we binned each light-curve using a 50 point window (10 sec). During the binning process, we used the average time of the 50 data points as the time of the binned data.

We then removed the systematic variations that are common across light-curves of the same run. Such systematic variations, which we call *trends*, could be caused by airmass, temporary telescope vibrations, noise in CCD images, etc. To remove such trends, we applied the Photometric DeTrending algorithm (PDT, Kim et al. 2009) to each individual run. PDT first calculates the correlation between whole light-curves as a measure of similarity between light-curves. PDT then uses the hierarchical clustering algorithm (Jain et al. 1999) to group similar light-curves together and determines one *master-trend* per group by summing weighted light-curves in the group. Using the determined master-trends, PDT finally removes trends from each individual light-curve by minimizing the residual between the master-trends and the light-curve. For more details about PDT, see Kim et al. (2009).

Figure 1 shows an example of a TAOS δ Sct star's light-curve before and after detrending process. X-axis is time in minutes and y-axis is flux. As the figure shows, periodic signals are clearly recovered after detrending.

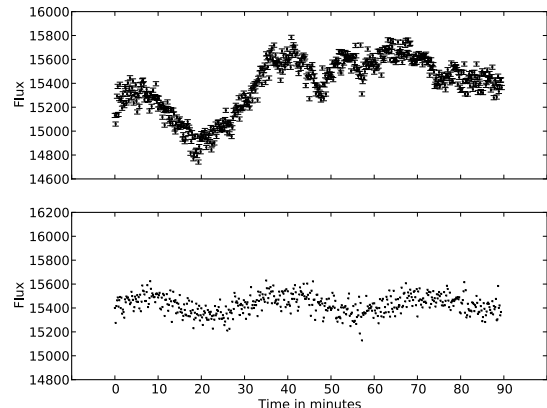


Fig. 1.— An example light-curve of a TAOS δ Sct star. X-axis is time in minutes and y-axis is flux. The top panel is the light-curve before detrending and the bottom panel is the light-curve after detrending. The periodic signals contaminated by unstable weather (e.g. moving clouds) are successfully recovered after detrending. We show the errors for each photometric measurement of the raw light-curve.

We show the errors for each photometric measurement before detrending, propagated from the errors estimated by the TAOS photometry pipeline (Zhang et al. 2009).

2.3. Detection of Short-Period Variable Stars

After we finished the preprocessing, explained in the previous section, we applied the Fast Fourier Transform algorithm (FFT; Brigham 1974) to each light-curve in order to detect periodic signals. Note that the individual measurements of TAOS light-curves are evenly spaced with a 5Hz sampling rate.² Thus FFT is appropriate for the detection of periodic signals. We focused on the detection of short-period variable stars whose periods are $\lesssim 1.5$ hour because TAOS monitors a given field for a maximum of 1.5 hours.

We describe the basic steps of the detection process below:

- We apply FFT to each detrended light-curve and derive the power spectrum of the light-curve. We then examine if there exists a frequency (or frequencies) whose power is bigger than five times the standard deviation of powers of the background frequencies. The standard deviation of powers is calculated after removing outliers using 3-sigma clipping.³ We identify the star as a variable candidate

¹During 2005 and 2006 observational season, one of the four TAOS telescopes was not operational.

²Binned light-curves are evenly spaced as well.

³Those outliers are only removed for the calculation of the standard deviation. They are included in the search of periodic signals.

if there is a frequency higher than five times the standard deviation.

- For each candidate variable we check if the periodic signal is detected on the other telescopes' light-curves of the same run. If it is not detected by the other telescopes, we remove the star from the candidate list.
- We visually inspect all raw zipper images for the candidates and remove false positives caused by moving asteroids, photometry defects or other contamination due to various noise sources. For instance, the flux of stars in the neighborhood of fast moving objects could be increased and decreased within an hour, which resembles periodic signals.
- We cross-match all of the candidates with SIMBAD (Wenger et al. 2000) and remove the false positives that are confirmed to be other types of variable stars (e.g. eclipsing binary stars).
- Finally we remove the variable stars whose periods are longer than 1.5 hours.

3. Detection Results

With the detection algorithm described in the previous section, we found 41 δ Sct candidate stars whose periods are shorter than 1.5 hours and whose amplitudes are within a few hundredth of a magnitude (hereinafter, TAOS δ Sct stars). Among those 41 TAOS δ Sct stars, one of them is a previously *suspected* variable star, NSV 3816, from the Suspected Variable stars and Supplement (Samus et al. 2009). However, the period and amplitude of NSV 3816 have never been published before. The remaining 40 TAOS δ Sct stars are newly detected by this study.

After the TAOS δ Sct stars were identified, we extracted the physical parameters of each star by cross-matching them with various astronomical catalogs. We show catalogs we used in Table 1. We found that 12 of the detected 41 TAOS δ Sct stars have spectral types from A0 to F5, which are typical spectral types for δ Sct stars. Unfortunately the rest of them, except for two peculiar δ Sct stars -discuss in Section 3.3-, do not have spectral information. Nevertheless, their short period and low amplitude strongly suggest that they are LADS rather than other types of variables, such as RR Lyrae or Cepheids, whose periods and amplitudes are relatively longer and larger than those of δ Sct stars.

As a byproduct of our analysis, we detected a previously known variable star with δ Sct pulsation, GM Leo, which is actually a λ Bootis star (Handler et al. 2000). Some λ Bootis stars show δ Sct pulsations (Paunzen 2004) and can have spectral types from late B to early F, which makes it difficult to distinguish them

from δ Sct stars. In such cases, there are no clear differences between δ Sct stars and λ Bootis stars except the metal abundance (Balona 2004); λ Bootis stars show weak metal lines such as Mg II λ 4481 line (Paunzen 2004).

We also checked several preexisting catalogs of δ Sct stars to see if there are previously known δ Sct stars in the TAOS observation fields. Table 2 shows the preexisting catalogs we checked. As a result of this search, we found only one previously known δ Sct pulsation star to be in the TAOS observation fields. That turns out to be GM Leo, which as we mentioned above, we successfully detected. Although GCVS classified GM Leo as δ Sct star based on the work by Handler et al. (2000), Handler et al. (2000) in their paper claimed GM Leo is not a δ Sct star but a λ Bootis star. Thus we removed GM Leo from our detection list.

3.1. List of the Detected 41 δ Sct Stars

Table 3 shows the 41 TAOS δ Sct stars' physical information such as positions, magnitudes, frequencies, amplitudes, spectral types, etc.

We used the FFT algorithm to detect periodic signals however we used PERIOD04 to derive their physical parameters such as period and amplitude.⁴ This is because PERIOD04 improves the frequency by fitting the light-curve with a combination of sine curves. Moreover PERIOD04 also provides errors for the derived frequencies. Figure 2 shows a comparison result of power spectra derived from an FFT method and PERIOD04 for a single TAOS δ Sct star. X-axis is frequency in counts/day, y-axis is scaled power. Solid line is power spectrum derived from an FFT method and dashed line is power spectrum derived from PERIOD04. As the figure shows, the two spectra are almost consistent.

As we mentioned in the previous section, TAOS operates multiple telescopes simultaneously monitoring the same patch of the sky. Thus we have a maximum of three simultaneous light-curves for all TAOS δ Sct stars for a given zipper run. To derive more precise frequencies and amplitudes, for each identified δ Sct star we summed the light-curves from each of the telescopes. Moreover, the TAOS telescopes occasionally visit same fields multiple times. In such cases, we merge all corresponding normalized light-curves⁵ of each identified δ Sct star into a single but longer light-curve. Having longer light-curves we were able to extract multiple frequencies using PERIOD04. Among the extracted frequencies, we selected the frequencies whose SNR is bigger than five. The SNR of each frequency was calculated using PERIOD04 as well.⁶ As a result we found 16 TAOS δ

⁴Since PERIOD04 gives half of the full amplitudes, we doubled amplitudes derived by PERIOD04 as Rodríguez et al. (2000) and other authors do.

⁵We normalized each light-curve by their mean values.

⁶Although other authors have suggested a threshold of SNR > 4

Table 1: Catalogs Used to Extract Additional Parameters

Catalog	Reference
GCVS	Perryman & ESA (1997)
All-Sky Compiled Catalogue of 2.5 million stars	Kharchenko (2001)
HD	Cannon & Pickering (1993)
Catalogue of Stellar Spectral Classifications	Skiff (2009)
Tycho-2 Catalogue of the 2.5 Million Brightest Stars	Høg et al. (2000)
Guide Star Catalog (GSC)	Lasker et al. (2008)
USNO-B 1.0	Monet et al. (2003)
SAO Star Catalog J2000	SAO Staff (1995)
Catalog of Projected Rotational Velocities	Glebocki & Stawikowski (2000)
Rotational Velocity Determinations for 118 δ Sct Variables	Bush & Hintz (2008)

Table 2: Preexisting Catalogs of δ Sct Stars

Catalog	Source Surveys	Number of δ Sct Stars	Reference
R2000 ^a	MACHO, OGLE, Hipparcos, etc	~600	(Rodríguez et al. 2000)
ROTSE ^b	ROTSE	6	(Jin et al. 2003)
ASAS ^c	ASAS	~500	(Pojmanski et al. 2006)
GCVS ^d	various surveys	~500	(Samus et al. 2009)
TAOS	TAOS	41	this paper
Others			
	5 new γ Doradus and 5 new δ Sct survey	5	(Henry et al. 2001)
	Case study for HD 173977	1	(Chapellier et al. 2004)
	Case study for HD 8801	1	(Henry & Fekel 2005)
	The first HADS in an eclipsing binary star	1	(Christiansen et al. 2007)
	Variable stars in NGC 2099	9	(Kang et al. 2007)
	Transit survey of M37	2	(Hartman et al. 2008)
	ASAS variable stars in the Kepler field of view	4	(Pigulski et al. 2009)

^a The catalog compiled by Rodríguez et al. (2000)

^b Robotic Optical Transient Search Experiment.

^c All-Sky Automated Survey.

^d General Catalog of the Variable Stars.

Sct stars having multiple frequencies (see Table 3). Note that we did not attempt to extract multiple frequencies if the star is detected only once (i.e. detected in only single zipper run). It is also worth mentioning that we lose detectability on relatively long period pulsations because we normalized the light-curves while merging them.

All detected δ Sct stars are relatively bright as shown in the table (the faintest star's m_V is around 12). This is because the limiting magnitude of TAOS *zipper mode* is relatively bright at ~ 13.5 (Lehner et al. 2009) and also because high SNR is needed to detect low-amplitude variations of a few milli-magnitude. To find m_V , m_B and spectral types, we used Centre de Données astronomiques de

Strasbourg (CDS) web service (Genova et al. 2000).

In Table 3, we also provide the number of the total observations (i.e. the number of the total zipper runs) and the number of identifications by the FFT analysis for each TAOS δ Sct star. Since the TAOS telescopes observe same fields multiple times, we have multiple light-curves for stars in the fields. Note that we applied the FFT algorithm to each light-curve to detect periodic signals. Nevertheless, as the table shows, not every light-curve of the TAOS δ Sct stars were confirmed to have periodic signals. This is mainly because of the poor quality of some of the light-curves caused by trends and noise (i.e. unstable weather, telescope vibration, etc). Although we removed most of the trends using PDT, it is nearly impossible to recover the intrinsic periodic signal of a few milli-magnitude in the presence of large systematic errors.

(Breger et al. 1993; Christiansen et al. 2007), we empirically found that a threshold of $\text{SNR} > 4$ produces false positives and thus we set the SNR threshold to five.

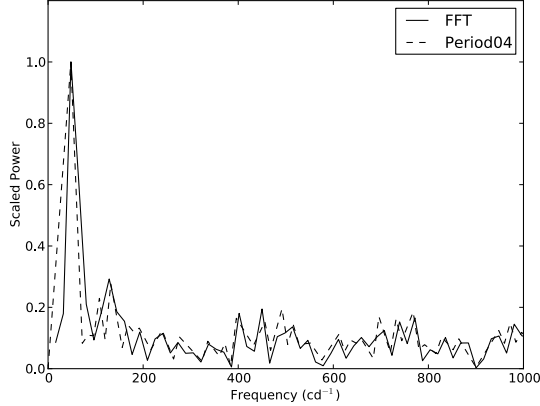


Fig. 2.— A comparison result of power spectrum derived from an FFT method and from PERIOD04. X-axis is frequency in counts/day, y-axis is scaled power. Solid line is the power spectrum derived from an FFT method and dashed line is the power spectrum derived from PERIOD04. The two spectra appear almost identical.

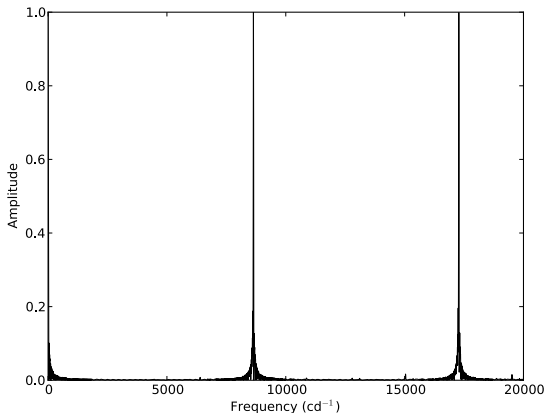


Fig. 3.— An example of a spectral window of a single zipper run. Peaks with regular intervals (two times of the Nyquist frequency) appear because points are equally spaced in a single zipper run.

3.2. Spectral Windows and Power Spectra of TAOS δ Sct Stars

In Figure 3 we show an example of a spectral window of a single zipper run. Since the observational times are almost equally spaced, peaks with regular intervals (two times the Nyquist frequency) are present in the spectral window (Deeming 1975). The Nyquist frequency is 4320Hz since the gap between each consecutive binned data is 10 sec.

Figure 4, 5 and 6 show the spectral windows along with the power spectra of three TAOS δ Sct stars. Stars included in the figures are 020.00141 (Figure 4), 121.00043 (Figure 5) and 054.00014 (Figure 6). The top panels in each figure show the spectral windows and the bottom panels (and the middle panel in Figure 6) show the power spectra of the stars. Dashed lines indicate the detected frequencies. Note that we improved the detected frequencies by fitting a combination of sine waves using PERIOD04. Thus the improved frequencies could be slightly shifted from the original peaks in the power spectra (e.g. see the bottom left panel in Figure 4) after the fitting.

As Table 3 shows, the star with ID 020.00141 was identified only once and is relatively fainter ($m_V = 11.40$) than other TAOS δ Sct stars. Its amplitude is one of the smallest amplitudes and its detected frequency SNR is the lowest among TAOS δ Sct stars. Thus the power spectrum of this star represents one of the “worst case scenario”. We detected one single frequency for this star. The star with ID 121.00043 was identified three times and is relatively bright ($m_V = 9.13$). The spectral window and the power spectrum of the star could represent a “moderate-level scenario”. We detected one frequency for this star. Finally, the star with ID 054.00014 was identified nine times and is relatively bright ($m_V = 9.50$). Thus its spectral window and power spectrum represents one of the “best case scenario”. Using PERIOD04, we detected three frequencies for this star. As can be seen from the figures, there are no significant peaks in the spectral windows at the detected frequencies.

3.3. Spectroscopy of Two Peculiar Spectral Type δ Sct Stars

As we mentioned in the previous section, we found two peculiar spectral type δ Sct stars which have B8 and G5 spectral types. These are the bluest and reddest spectral types of δ Sct stars ever detected. The spectral type of the B8 star was extracted from the Henry Draper Catalogue and Extension (HD, Cannon & Pickering 1993). Unfortunately we could not find any spectroscopic literature for the G5 star so we suspect that the spectral type is most likely derived from its color information. The spectral type of the G5 star was extracted from SIMBAD. To confirm their spectral types, we observed the two stars with spectroscopic instruments.

For the B8 star, we used the BOES⁷ of the 1.8-m telescope at the Bohyunsan Optical Astronomy Observatory (BOAO), South Korea (Kim et al. 2007). We used IRAF (Tody 1986, 1993) for the reduction of the obtained spectroscopic data. Figure 7 shows the normalized spectrum of the B8 candidate star. We indicate several important spectral lines in the figure. As the figure shows, Ca II K line is very strong which is typical for A type stars (Gray

⁷BoaO Echelle Spectrograph

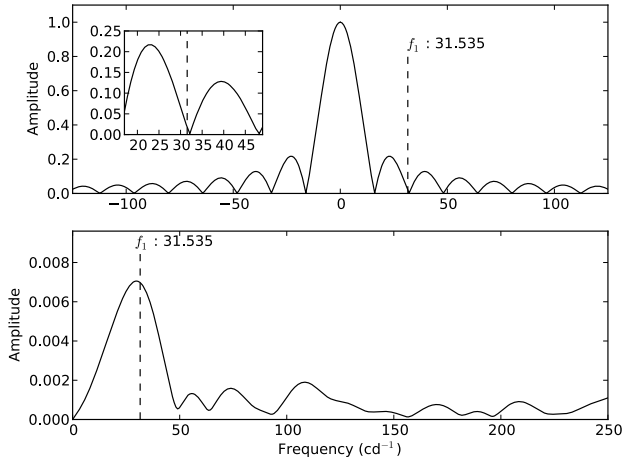


Fig. 4.— The spectral window and the power spectrum of the star ID 020.00141. The top panel shows the spectral window and the bottom panel shows the power spectrum of the star. The dashed line shows the detected frequency. In the top panel, we magnified the spectral window to clearly show the detected frequency.

& Garrison 1987). B type stars do not show such strong Ca II K line. The spectrum also shows weak metallic lines (e.g. Ca I and Mg II line) which are usually presented in A type stars. Based on the strength of Ca II K line, hydrogen lines and metallic lines, the star is likely an A5 type star although the classification of sub-class is rather uncertain due to the low SNR of the spectrum.

In addition, to observe the G5 star, we used the FAST instrument mounted at the Fred Lawrence Whipple Observatory (FLWO) 1.5m telescope, Mount Hopkins in Arizona (Fabricant et al. 1998). After comparing the observed data with standard spectral libraries (Pickles 1998), we found that the spectral type of the star is not a G5 but an F0. Therefore the star is likely a typical δ Sct star.

4. Summary

We analyzed the TAOS 2-year data accumulated during 2005 and 2006 observations in order to find short-period variables. Using the TAOS photometry pipeline we created photometric light-curves. We removed systematic trends commonly appeared in the light-curves using PDT. To detect periodic signals in the detrended light-curves, we applied the Fast Fourier Transform (FFT) to each light-curve. FFT is a simple but *powerful* algorithm for detection of periodic signals when data points are evenly spaced. We then chose light-curves which possess a frequency (or frequencies) whose power is five times larger than the standard deviation of powers of all background frequencies in the power

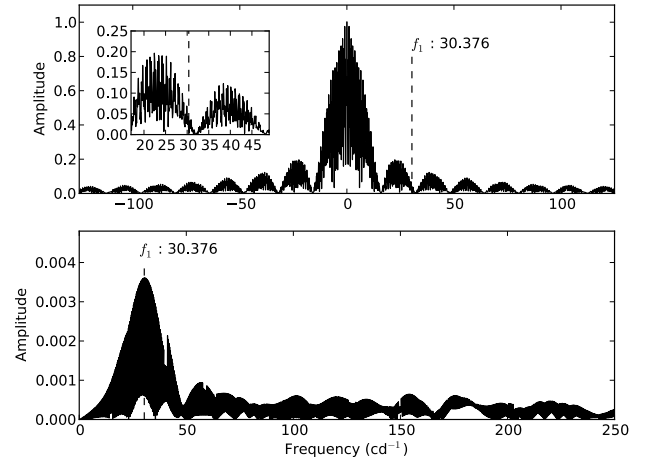


Fig. 5.— The spectral window and the power spectrum of the star ID 121.00043. The top panel shows the spectral window and the bottom panel shows the power spectrum of the star. The dashed line shows the detected frequency. In the top panel, we magnified the spectral window to clearly show the detected frequency.

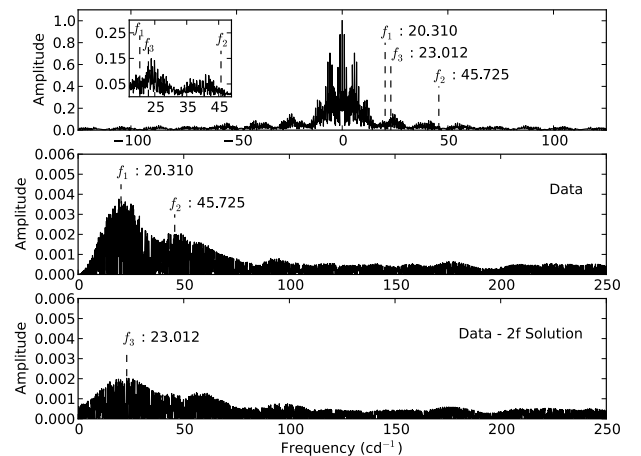


Fig. 6.— The spectral window and the power spectrum of the star ID 054.00014. We detected three frequencies (dashed lines) using PERIOD04. The top panel shows the spectral window. The middle panel shows the first two frequencies. The bottom panel is the power spectrum after whitening the two frequencies. In the top panel, we magnified the spectral window to clearly show the detected frequencies.

spectrum derived using FFT. We visually checked the light-curves and raw images of all candidates to remove false positives caused by moving asteroids, photometry

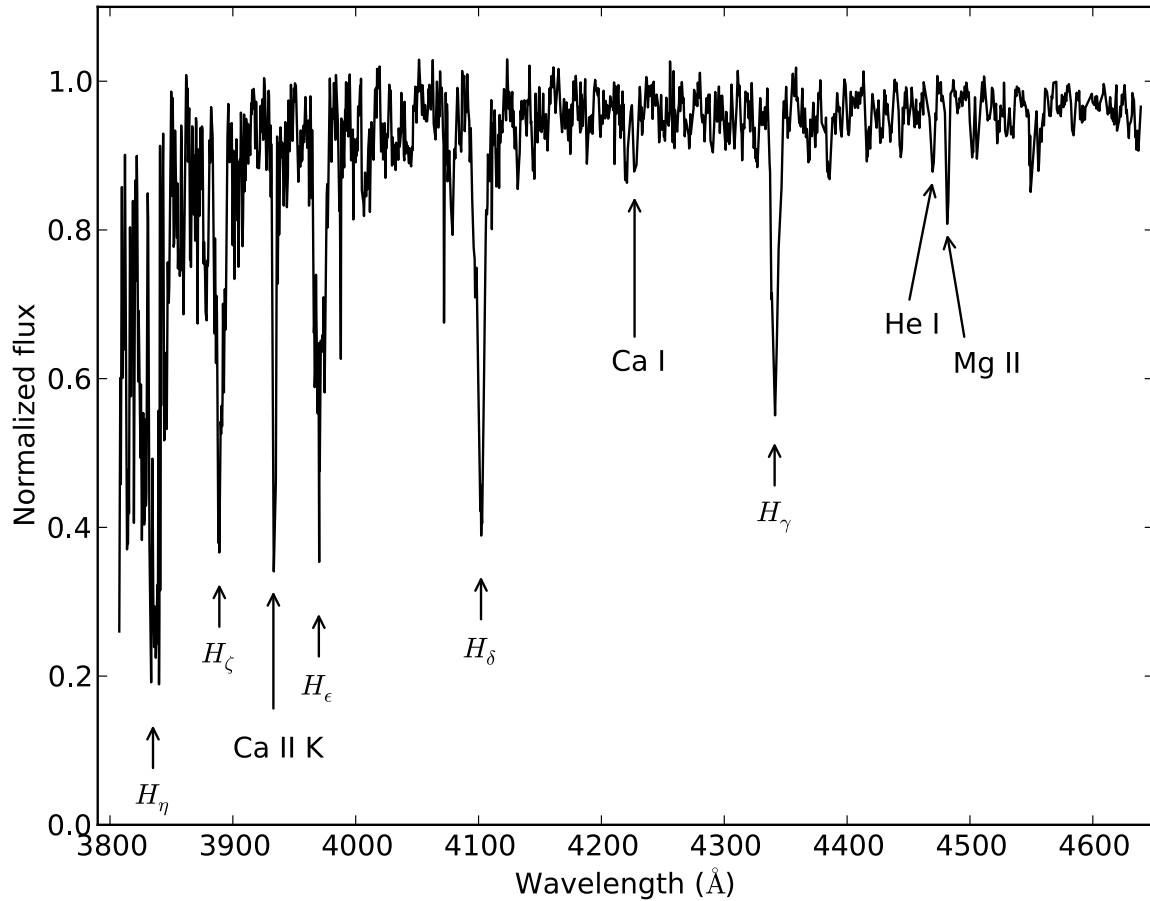


Fig. 7.— The normalized spectrum of the B8 candidate star. There are strong Ca II K line and weak metallic lines, which is typical for A type stars. The star is likely an A5 type star rather than a B8 type star.

defects, etc. We also removed candidates which were detected by only one of the three telescopes. All remaining 41 variable candidates have periods about an hour and amplitudes less than a few hundredth of a magnitude, which strongly suggests that they are low-amplitude δ Sct stars (LADS).

We cross-matched the detected δ Sct candidate stars with many astronomical catalogs to extract additional information (e.g. magnitude, spectral type, variability type, etc). As a result we found that 14 stars have spectral types from A to F, which are typical spectral types for δ Sct stars. The rest of the detected δ Sct stars do not have spectral information.

The light-curves of TAOS δ Sct stars are accessible at the Time Series Center (TSC, <http://timemachine.iic.harvard.edu>). Initiative in Innovative Computing (IIC) at Harvard. PERIOD04 project files of each star is also provided. The project files contain complete light-curve data, power

spectrum, frequency and amplitude information.

Acknowledgements

Y.-I. Byun acknowledges the support of National Research Foundation of Korea through Grant 2009-0075376. The work at National Central University was supported by the grant NSC 96-2112-M-008-024-MY3. Work at Academia Sinica was supported in part by the thematic research program AS-88-TP-A02. Work at the Harvard College Observatory was supported in part by the National Science Foundation under grant AST-0501681 and by NASA under grant NNG04G113G. SLM's work was performed under the auspices of the U.S. Department of Energy by Lawrence Livermore National Laboratory in part under Contract W-7405-Eng-48 and by Stanford Linear Accelerator Center under Contract DE-AC02-76SF00515. K. H. Cook's work was performed under the auspices of the U.S. Department of Energy by

Lawrence Livermore National Laboratory in part under Contract W-7405-Eng-48 and in part under Contract DE-AC52-07NA27344. We also thanks J. D. Hartman at Harvard-Smithsonian Center for Astrophysics for useful discussion.

The detrending and the analysis of datasets in this paper were run on the Odyssey cluster supported by the FAS Research Computing Group at the Harvard. This research has made use of the SIMBAD database, operated at CDS, Strasbourg, France. IRAF is distributed by the National Optical Astronomy Observatories, which are operated by the Association of Universities for Research in Astronomy, Inc., under cooperative agreement with the National Science Foundation.

REFERENCES

- Alcock C., Dave R., Giammarco J., et al. 2003, *Earth Moon and Planets*, 92, 459
- Arentoft T., Sterken C., Handler G., et al. 2001, *A&A*, 374, 1056
- Balona L. A., 2004, in Zverko J., Ziznovsky J., Adelman S. J., Weiss W. W., eds, *The A-Star Puzzle Vol. 224 of IAU Symposium, Pulsations of A stars*. pp 325–334
- Balona L. A., Evers E. A., 1999, *MNRAS*, 302, 349
- Breger M., 2000a, in Breger M., Montgomery M., eds, *Delta Scuti and Related Stars Vol. 210 of Astronomical Society of the Pacific Conference Series, δ Scuti stars (Review)*. p. 3
- Breger M., 2000b, *MNRAS*, 313, 129
- Breger M., Lenz P., Antoci V., et al. 2005, *A&A*, 435, 955
- Breger M., Pamyatnykh A. A., 1998, *A&A*, 332, 958
- Breger M., Pamyatnykh A. A., Zima W., et al. 2002, *MNRAS*, 336, 249
- Breger M., Stich J., Garrido R., et al. 1993, *A&A*, 271, 482
- Brigham E. O., 1974, *The fast Fourier Transform*
- Brown T. M., Gilliland R. L., 1994, *ARA&A*, 32, 37
- Bruntt H., Suárez J. C., Bedding T. R., et al. 2007, *A&A*, 461, 619
- Bush T. C., Hintz E. G., 2008, *AJ*, 136, 1061
- Buzasi D. L., Bruntt H., Bedding T. R., et al. 2005, *ApJ*, 619, 1072
- Cannon A. J., Pickering E. C., 1993, *VizieR Online Data Catalog*, 3135, 0
- Chapellier E., Mathias P., Garrido R., et al. 2004, *A&A*, 426, 247
- Chen W. P., Alcock C., Axelrod T., et al. 2007, in Valsecchi G. B., Vokrouhlický D., Milani A., eds, *IAU Symposium Vol. 236 of IAU Symposium, Search for small trans-Neptunian objects by the TAOS project*. pp 65–68
- Christiansen J. L., Derekas A., Ashley M. C. B., et al. 2007, *MNRAS*, 382, 239
- de Boor C., 1978, *A practical guide to splines*. New York: Springer, p. 87-144
- Deeming T. J., 1975, *Ap&SS*, 36, 137
- Fabricant D., Cheimets P., Caldwell N., Geary J., 1998, *PASP*, 110, 79
- Garrido R., Garcia-Lobo E., Rodriguez E., 1990, *A&A*, 234, 262
- Genova F., Egret D., Bienaymé O., et al. 2000, *A&AS*, 143, 1
- Glebocki R., Stawikowski A., 2000, *Acta Astronomica*, 50, 509
- Gray R. O., Garrison R. F., 1987, *ApJS*, 65, 581
- Handler G., Gray R. O., Shobbrook R. R., 2000, *Information Bulletin on Variable Stars*, 4876, 1
- Hartman J. D., Gaudi B. S., Holman M. J., et al. 2008, *ApJ*, 675, 1254
- Henry G. W., Fekel F. C., 2005, *AJ*, 129, 2026
- Henry G. W., Fekel F. C., Kaye A. B., et al. 2001, *AJ*, 122, 3383
- Høg E., Fabricius C., Makarov V. V., et al. 2000, *A&A*, 355, L27
- Jain A. K., Murty M. N., Flynn P. J., 1999, *ACM Computing Surveys*, 31, 264
- Jin H., Kim S.-L., Kwon S.-G., et al. 2003, *A&A*, 404, 621
- Kang Y. B., Kim S.-L., Rey S.-C., et al. 2007, *PASP*, 119, 239
- Kharchenko N. V., 2001, *Kinematika i Fizika Nebesnykh Tel*, 17, 409
- Kim D.-W., Protopapas P., Alcock C., et al. 2009, *MNRAS*, 397, 558
- Kim K.-M., Han I., Valyavin G. G., et al. 2007, *PASP*, 119, 1052
- Lasker B. M., Lattanzi M. G., McLean B. J., et al. 2008, *AJ*, 136, 735
- Lehner M. J., Wen C.-Y., Wang J.-H., et al. 2009, *PASP*, 121, 138
- McNamara D. H., Clementini G., Marconi M., 2007, *AJ*, 133, 2752
- Monet D. G., Levine S. E., Canzian B., et al. 2003, *AJ*, 125, 984
- Moya A., Garrido R., Dupret M. A., 2004, *A&A*, 414, 1081
- Paunzen E., 2004, in Zverko J., Ziznovsky J., Adelman S. J., Weiss W. W., eds, *The A-Star Puzzle Vol. 224 of IAU Symposium, The λ Bootis stars*. pp 443–450
- Perryman M. A. C., ESA eds, 1997, *The HIPPARCOS and TYCHO catalogues. Astrometric and photometric star catalogues derived from the ESA HIPPARCOS Space Astrometry Mission Vol. 1200 of ESA Special Publication*
- Pickles A. J., 1998, *PASP*, 110, 863
- Pigulski A., Pojmański G., Pilecki B., et al. 2009, *Acta Astronomica*, 59, 33

- Pojmanski G., Maciejewski G., Pilecki B., et al. 2006, VizieR Online Data Catalog, 2264, 0
- Pribulla T., Rucinski S., Matthews J. M., et al. 2008, MNRAS, 391, 343
- Ripepi V., Marconi M., Bernabei S., et al. 2003, A&A, 408, 1047
- Rodríguez E., López-González M. J., 2000, A&A, 359, 597
- Rodríguez E., López-González M. J., López de Coca P., 2000, A&AS, 144, 469
- Rodríguez E., Rolland A., López de Coca P., et al. 1996, A&A, 307, 539
- Samus N. N., Durlevich O. V., et al. 2009, VizieR Online Data Catalog, 1, 2025
- SAO Staff 1995, VizieR Online Data Catalog, 1131, 0
- Skiff B. A., 2009, VizieR Online Data Catalog, 1, 2023
- Tody D., 1986, in Crawford D. L., ed., Society of Photo-Optical Instrumentation Engineers (SPIE) Conference Series Vol. 627 of Presented at the Society of Photo-Optical Instrumentation Engineers (SPIE) Conference, The IRAF Data Reduction and Analysis System. p. 733
- Tody D., 1993, in Hanisch R. J., Brissenden R. J. V., Barnes J., eds, Astronomical Data Analysis Software and Systems II Vol. 52 of Astronomical Society of the Pacific Conference Series, IRAF in the Nineties. p. 173
- Wenger M., Ochsenbein F., Egret D., et al. 2000, A&AS, 143, 9
- Zhang Z. W., Kim D. W., Wang J. H., et al. 2009, PASP, 121, 1429
- Zima W., Breger M., Bischof K., et al. 2002, in Aerts C., Bedding T. R., Christensen-Dalsgaard J., eds, IAU Colloq. 185: Radial and Nonradial Pulsations as Probes of Stellar Physics Vol. 259 of Astronomical Society of the Pacific Conference Series, The Delta Scuti Network: Steps Towards Successful Asteroseismology of Delta Scuti Stars. p. 598

Table 3:: TAOs δ Sct stars in TAOs 2-year Data

No	ID ^a	RA (hh:mm:ss)	Dec (dd:mm:ss)	m_V	m_B	Frequency (cd^{-1})	Δm_V^b (mmag)	SNR ^c	Epoch (MJD)	Spectral Type	#/# ^d	Note
1	124.00003	00:52:40	+06:39:55	8.89	9.20	$24.421 \pm 3.975e^{-4}$	3.83 ± 0.20	6.5	53626.7469	A2	4 / 7	
2	038.00124	02:56:54	+34:23:20	11.60	12.00	$23.598 \pm 4.775e^{-1}$	7.95 ± 0.44	11.9	53678.6909		1 / 2	
3	053.00009	03:37:02	+18:21:51	8.48	8.80	$20.544 \pm 2.314e^{-4}$	5.99 ± 0.14	18.5	53671.7396	A2	3 / 8	
4	059.00115	03:42:41	+17:55:01	12.12	12.60	$25.836 \pm 7.587e^{-4}$	9.19 ± 0.68	13.6	54021.6614		3 / 8	
						$32.116 \pm 8.434e^{-4}$	7.97 ± 0.66	11.8	54021.6579			
						$12.034 \pm 1.291e^{-3}$	4.94 ± 0.58	7.5	54021.5979			
						$40.403 \pm 1.713e^{-3}$	3.53 ± 0.62	5.25	54021.6523			
5	059.00005	03:46:01	+18:34:00	9.14	9.46	$33.115 \pm 2.022e^{-4}$	8.00 ± 0.20	15.7	54006.7013	A5	7 / 8	B8 ^e
6	049.00056	04:03:21	+19:21:31	10.91	11.48	$18.068 \pm 4.793e^{-4}$	3.26 ± 0.20	6.4	54006.7020		6 / 16	
						$24.205 \pm 3.694e^{-4}$	9.15 ± 0.34	13.7	54029.8147			
						$17.761 \pm 6.312e^{-4}$	4.98 ± 0.36	7.5	54029.7806			
						$29.544 \pm 8.243e^{-4}$	4.00 ± 0.34	6.0	54029.8094			
7	068.00053	04:30:06	+20:55:00	11.45	12.36	$32.504 \pm 2.402e^{-5}$	10.17 ± 0.28	15.5	53643.8513	F0	8 / 15	G5 ^f
						$26.117 \pm 5.939e^{-5}$	4.10 ± 0.28	6.24	53643.8542			
8	060.00151	04:48:37	+21:10:33	11.44	11.64	$43.180 \pm 3.709e^{-4}$	5.13 ± 0.26	8.4	54012.7340	F5	6 / 32	
9	022.00001	04:56:14	+21:34:20	7.34	7.70	$21.582 \pm 1.709e^{-4}$	3.97 ± 0.12	12.9	54021.7647	F0	7 / 25	
						$21.146 \pm 3.268e^{-4}$	2.15 ± 0.12	6.94	54021.7495			
						$40.637 \pm 4.339e^{-4}$	1.57 ± 0.12	5.12	54021.7926			
10	020.00206	05:08:38	+22:49:37	11.85	12.16	$53.575 \pm 5.075e^{-1}$	7.62 ± 0.46	9.9	53705.6765		1 / 3	
11	020.00141	05:09:24	+23:16:05	11.40	12.29	$31.535 \pm 6.862e^{-1}$	6.87 ± 0.52	5.7	53705.6877		1 / 3	
12	021.00011	05:09:40	+21:50:05	8.99	9.21	$41.754 \pm 1.493e^{-4}$	8.05 ± 0.18	17.7	53975.7771		5 / 7	
						$37.264 \pm 4.476e^{-4}$	2.73 ± 0.18	5.9	53975.7883			
13	020.00135	05:10:14	+23:01:24	10.90	11.78	$39.254 \pm 6.865e^{-1}$	5.11 ± 0.40	6.3	53705.6974		1 / 3	
14	024.00234	05:15:19	+22:53:41	11.93	12.39	$25.804 \pm 2.471e^{-1}$	35.35 ± 1.04	12.8	53679.7864		1 / 2	
15	160.00106	06:01:30	+21:27:38	10.38	10.69	$21.063 \pm 3.878e^{-4}$	7.44 ± 0.22	13.9	53680.8125		3 / 8	
16	160.00004	06:04:05	+21:29:39	7.81	7.97	$25.827 \pm 5.607e^{-4}$	4.70 ± 0.16	15.5	53680.8193		3 / 8	
						$22.395 \pm 7.432e^{-4}$	3.55 ± 0.14	11.7	53680.8406			
						$38.868 \pm 1.077e^{-3}$	1.59 ± 0.12	5.2	53680.8298			
17	160.00199	06:04:26	+21:21:55	10.96	11.16	$43.741 \pm 9.070e^{-4}$	4.12 ± 0.26	11.0	53680.8119		3 / 8	
18	052.00132	07:39:07	+21:39:20	11.14	11.67	$23.802 \pm 3.343e^{-3}$	4.69 ± 0.30	7.2	53699.7766		2 / 3	
19	052.00069	07:39:09	+20:48:41	10.43	10.85	$21.288 \pm 7.664e^{-4}$	7.51 ± 0.28	11.6	53682.7645		3 / 3	
						$29.627 \pm 1.666e^{-3}$	3.41 ± 0.28	5.2	53682.7835			
20	052.00159	07:39:20	+21:11:22	11.25	11.59	$18.793 \pm 2.293e^{-3}$	9.59 ± 0.42	18.8	53699.7682		2 / 3	
						$27.366 \pm 3.345e^{-3}$	6.69 ± 0.42	13.4	53699.7680			
						$41.107 \pm 6.306e^{-3}$	3.19 ± 0.32	6.2	53699.7687			
21	054.00014	07:56:31	+21:52:29	9.50	9.74	$20.310 \pm 6.086e^{-5}$	2.89 ± 0.14	8.5	53702.8142	A5	9 / 19	NSV 3816
						$45.725 \pm 7.022e^{-5}$	2.16 ± 0.14	6.3	53702.8211			

Continued on next page

Table 3 – continued from previous page

No	ID ^a	RA (hh:mm:ss)	Dec (dd:mm:ss)	m_V	m_B	Frequency (cd ⁻¹)	Δm_V^b (mmag)	SNR ^c	Epoch (MJD)	Spectral Type	#/# ^d	Note
22	054.00075	07:58:27	+21:36:24	10.80	11.11	$23.012 \pm 7.570e^{-5}$	2.32 ± 0.14	6.8	53702.8130			
23	064.00006	08:43:26	+16:53:00	8.80	9.11	$22.591 \pm 3.776e^{-5}$	7.21 ± 0.026	12.9	53702.8148			5 / 19
24	064.00050	08:43:45	+17:25:00	10.60	10.94	$19.763 \pm 3.791e^{-1}$	6.84 ± 0.34	8.3	53812.5164			1 / 2
25	066.00003	08:44:07	+15:55:51	8.56	8.71	$20.148 \pm 4.392e^{-1}$	7.47 ± 0.44	8.6	53812.5238			1 / 2
26	062.00060	09:05:56	+17:47:27	10.90	11.50	$54.890 \pm 9.400e^{-1}$	6.37 ± 0.38	10.6	53774.6133	A0		1 / 2
27	062.00030	09:09:53	+17:41:08	10.18	10.40	$38.163 \pm 8.580e^{-4}$	11.24 ± 0.70	7.4	53753.6878	A5		3 / 9
28	107.00023	13:10:39	-06:25:01	10.25	10.51	$46.333 \pm 1.213e^{-3}$	7.94 ± 0.68	5.2	53753.7126			
29	099.00087	15:58:40	-19:27:14	11.62	12.46	$21.098 \pm 3.614e^{-5}$	7.64 ± 0.22	9.0	53753.6725			4 / 9
30	148.00060	16:51:54	+07:36:44	10.80	11.10	$20.214 \pm 1.921e^{-4}$	10.58 ± 0.30	10.4	53767.8800	A0		4 / 10
31	012.00024	19:51:31	-22:23:03	9.84	10.20	$19.673 \pm 3.479e^{-1}$	19.86 ± 0.92	12.4	53903.6396			1 / 1
32	153.00128	20:04:47	-20:32:05	11.63	12.34	$24.652 \pm 4.632e^{-4}$	27.71 ± 0.64	14.3	53812.7968	A5		2 / 12
33	121.00214	21:01:43	+16:39:37	11.20	11.57	$27.102 \pm 7.279e^{-1}$	8.22 ± 0.78	6.0	53959.6073	A6III		1 / 4
34	121.00043	21:03:25	+15:21:26	9.13	17.53	$19.313 \pm 5.077e^{-1}$	43.72 ± 2.92	6.4	53919.7373			1 / 1
35	028.00439	21:54:03	+25:11:07	12.85	13.54	$23.471 \pm 6.650e^{-4}$	9.20 ± 0.48	6.2	53559.7694			2 / 10
36	028.01026	22:01:08	+24:44:33	13.01	13.42	$30.376 \pm 1.866e^{-3}$	3.61 ± 0.16	12.8	53750.7027			3 / 10
37	003.00147	22:01:53	-12:28:52	12.24	12.23	$19.445 \pm 6.747e^{-5}$	32.02 ± 1.16	18.4	53575.7487			5 / 9
38	138.00022	22:05:55	+28:02:32	9.54	10.05	$21.088 \pm 1.405e^{-4}$	15.39 ± 1.02	8.8	53575.7599			
39	138.00110	22:09:41	+28:12:40	10.80	11.30	$8.847 \pm 1.238e^{-3}$	9.79 ± 1.02	5.7	53575.7475			5 / 9
40	030.00019	22:59:23	+37:14:33	9.26	9.65	$33.008 \pm 5.843e^{-5}$	36.45 ± 1.72	11.5	53575.7736			4 / 4
41	030.00195	23:02:06	+36:30:28	11.51	11.91	$17.731 \pm 2.283e^{-4}$	32.24 ± 1.14	18.5	53947.6845			
42						$41.446 \pm 1.392e^{-3}$	12.43 ± 1.28	7.4	53947.7181			
43						$30.608 \pm 8.642e^{-4}$	9.26 ± 1.26	5.4	53947.7213	A3		6 / 13
44						$17.767 \pm 6.301e^{-5}$	5.11 ± 0.20	12.0	53781.7689			
45						$18.090 \pm 9.286e^{-5}$	3.50 ± 0.20	8.2	53781.7733			
46						$16.877 \pm 1.751e^{-4}$	7.87 ± 0.32	12.6	53584.7897			4 / 13
47						$20.199 \pm 9.589e^{-4}$	5.21 ± 0.20	13.5	53657.6049	F2		4 / 8
48						$29.390 \pm 1.564e^{-3}$	2.60 ± 0.18	6.7	53657.6029			
49						$19.757 \pm 1.579e^{-3}$	2.86 ± 0.20	7.4	53657.5702			
50						$22.278 \pm 5.635e^{-4}$	13.56 ± 0.42	21.4	53657.5695			5 / 8
51						$18.802 \pm 1.529e^{-3}$	5.14 ± 0.40	8.1	53657.6120			

^a Combination of TAOS field ID and TAOS star ID.^b We doubled amplitudes derived by PERIOD04.^c SNR of frequencies derived using PERIOD04.^d The number of identifications / the number of zipper runs. Note that we did not count zipper runs observed by only one telescope.^e The B8 star found to be an A5 star as explained in the text.^f The G5 star found to be an F0 star as explained in the text.